Datasheet

Handheld Hyperspectral Imager | ATH2500

Features:

- Range: 400 ~ 1000 nm, 400 ~ 1700 nm
- Snapshot Imaging
- Max. Spatial Res.: 2048×1088, 1280×1084
- Android System
- 5.0 Inch HD touch screen
- Super Imaging Quality
- Data format compatible ENVI
- Size: 132mm ×99mm × 65mm
- Weight： 920g、1760g

Application

- Prospecting for geology and minerals
- Agriculture Monitoring: Crop condition and yield assessment
- Forest pest and fire prevention monitoring
- Coastline and ocean monitoring
- Pasture monitoring
- Lake and watershed monitoring
- Remote sensing teaching and research
- Industrial sorting
- Ecological environment protection and mine monitoring
- Water quality and soil monitoring

Description:

ATH2500 features handheld imaging imager with optimized new design. It's compact size and light weight, one hand to held to operate Android system, hand touch screen, built-in big memory fit for high quality images combined high spatial resolution, spectral resolution, and wide range.

ATH2500 consists of two parts of hyperspectral camera and lens.

ATH-4-10 uses 1920*1200 pixels excellent CCD imager with clear images, low noise, good linearity.

ATH2500-4-17 uses SWIR cooled down to -15℃ with super SNR.

ATH 2500 designed stable temperature optical bench can ensure stability and sensitivity. They are widely applied to lab, field, industries in the agriculture, forestry, satallite, and remote sensing etc.

Models	Description
ATH2500-4-10	400~1000 nm， standard version
ATH2500-4-17	400~1700 nm， standard version

1503 Bld. A04, 3rd Software Park, Jimei, Xiamen, 361005, China
Tel: +86-592-6102588

1. ATH2500 Hyperspectral Camera Series

ATH2500系列	特征	主要应用领域
ATH2500	400~1000nm VIS-NIR Hyperspectral Camera	Precision agriculture, agroforestry diseases and insect pests, vegetation analysis, planting area assessment, crop yield assessment, water quality analysis, art scanning, cultural relic identification, pattern scanning, industrial sorting, oil pollution detection, etc
ATH2500-4-17	0.4~1.7μm SWIR Hyperspectral Camera	Semiconductor, industrial sorting, food sorting, construction waste sorting, meat sorting, plastic sorting, geological exploration, mineral exploration, cultural relics identification, judicial identification, document inspection

2.Performance Parameter

	ITEM	PARAMETER	PARAMETER
	Model	ATH2500	ATH2500-4-17
1	Spectral Range	400 ~ 1000 nm	0.4~1.7μm
2	Spectral Channels	500	500
3	Spatial Channels	1920*1200	1280*1084
4	Sensor Type	High Sensitivity VNIR detector	Te-cooled InGaAs SWIR Detector
5	Image Resolution	1920*1200	1280 × 1084
6	Raw Pixels Size	5.86 μm × 5.86 μm	5 μm × 5 μm
7	Bit Depth	14 bits	14 bits
8	Frame Rate	162 fps	1150 fps
9	Scanning Type	Full-frame imaging	Full-frame imaging
10	OS	Android 8.0	
11	Touch Panel	5 -inch , capacitive touch screen （1280×720）	
12	Storage System	32GB（Standard）、64GB、128GB、256GB Optional	
13	Interface	USB2.0、WIFI、Bluetooth	
14	Physical interfaces	USB, Memory Cards,Tripods, Lanyards	
15	Buttons	Power button，Detection of key	
16	IP grade	IP54	
17	Battery span	>4H，Battery replaceable	
18	FOV	15.2°@f=35mm，Depending on the lens	
19	IFOV	0.7mrad@f=35mm，Depending on the lens	
20	Size	132mm ×99mm × 65mm	
21	Weight	920g	192mm ×168mm × 153mm
22	Working Temp.	-20 ~ 50°C	1760g
23	Storage Temp.	-30 ~ 70°C	

1503 Bld. A04, 3rd Software Park, Jimei, Xiamen, 361005, China
Tel: +86-592-6102588

3. ATH2500 Physical

1503 Bld. A04, 3rd Software Park, Jimei, Xiamen, 361005, China
Tel: +86-592-6102588

Figure 1 ATH2500 Physic

4. ATH2500 Hyperspectral Imaging

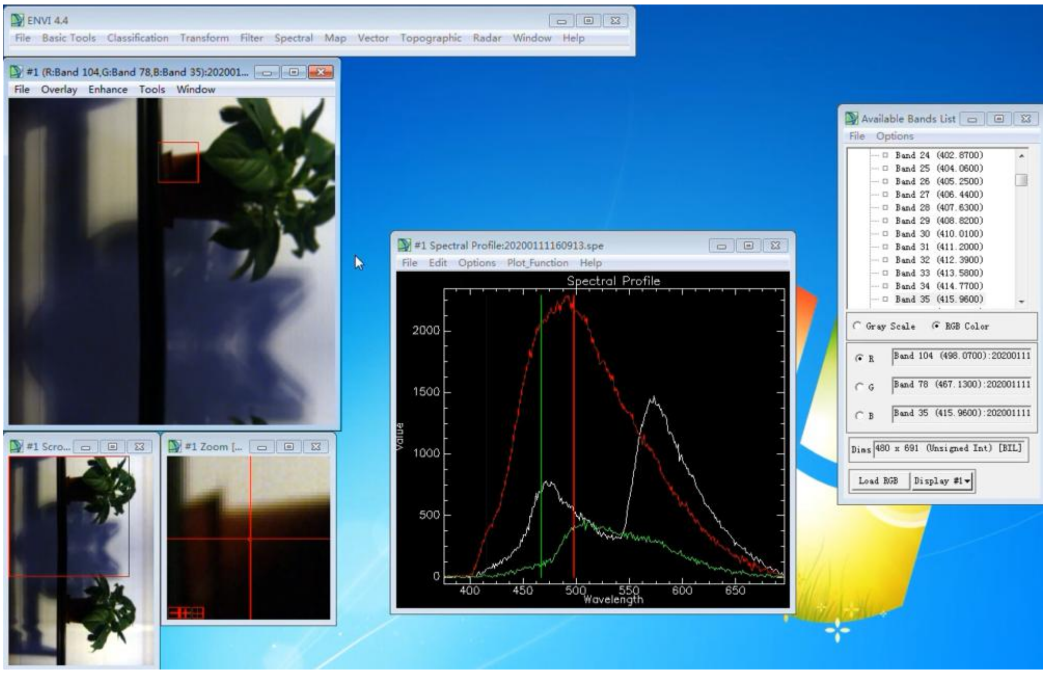

Figure 2 ATH2500 hyperspectral imaging

1503 Bld. A04, 3rd Software Park, Jimei, Xiamen, 361005, China
Tel: +86-592-6102588

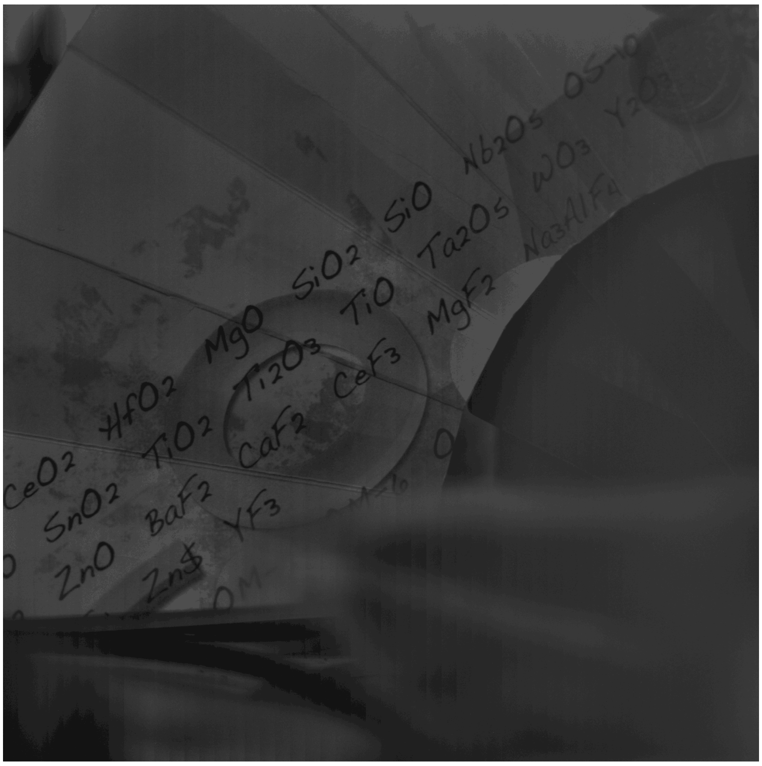

Figure 3 ATH2500 493nm band

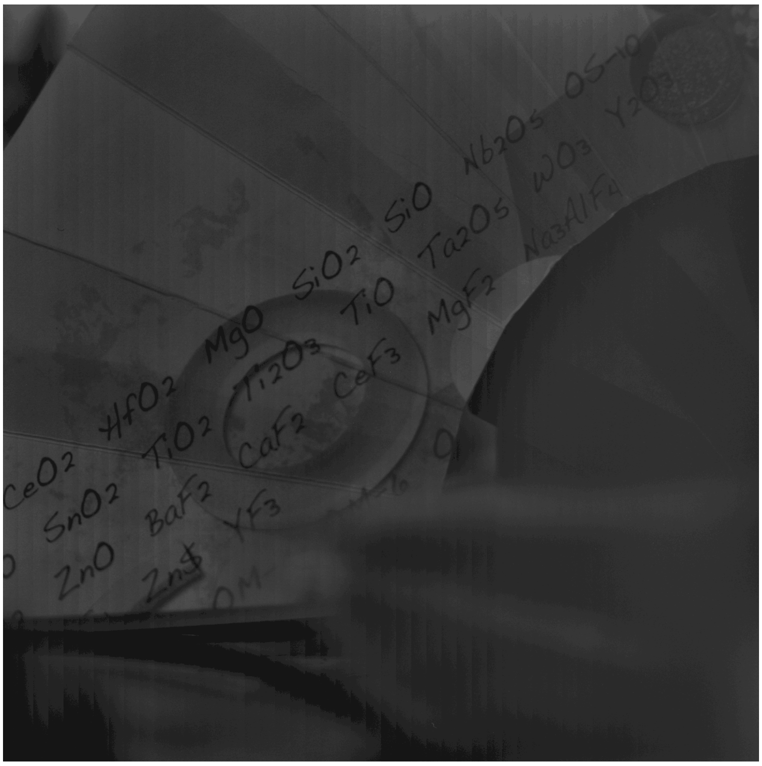

Figure 4 ATH2500 653nm band

1503 Bld. A04, 3rd Software Park, Jimei, Xiamen, 361005, China
Tel: +86-592-6102588

5.高光谱应用举例

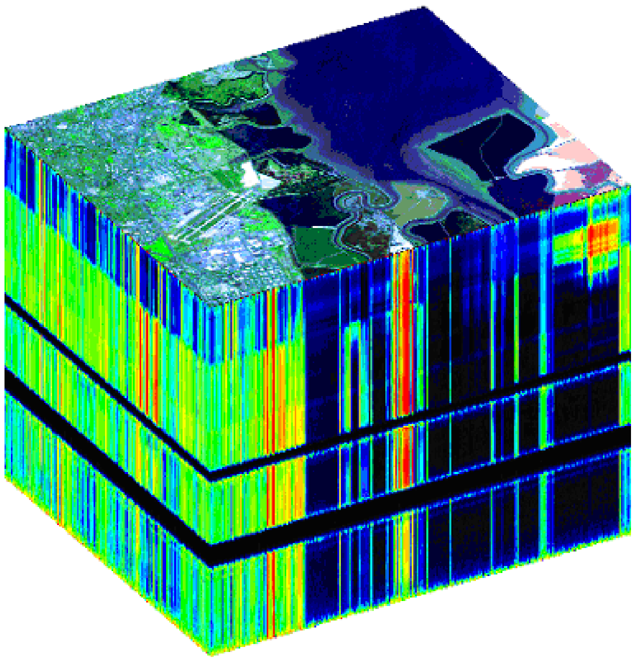

Figure 5 Data cube captured

Figure 6 Drone experiment

1503 Bld. A04, 3rd Software Park, Jimei, Xiamen, 361005, China
Tel: +86-592-6102588

Figure 7 Outdoor experiment scene Ⅰ

Figure 8 Outdoor experiment scene Ⅱ

1503 Bld. A04, 3rd Software Park, Jimei, Xiamen, 361005, China
Tel: +86-592-6102588


Figure 9 Outdoor experiment scene Ⅲ

Figure 10 Outdoor experiment scene Ⅳ

5.1 Industrial Sorting Application

With the development of NIR hyperspectral technology, such as Jiang tried to use near-infrared hyperspectral technology to detect impurities in cotton, especially the application of SWIR hyperspectral technology, which significantly improved the detection rate of plastic films compared with conventional methods.

Hyperspectral imaging technology is based on a very large number of narrow-band image data technology, which can obtain image information and spectral information of the sample while imaging the sample. Commonly used hyperspectral data processing methods include partial least squares (PLS),

1503 Bld. A04, 3rd Software Park, Jimei, Xiamen, 361005, China
Tel: +86-592-6102588

support vector machine (SVM) and artificial neural network (ANN).

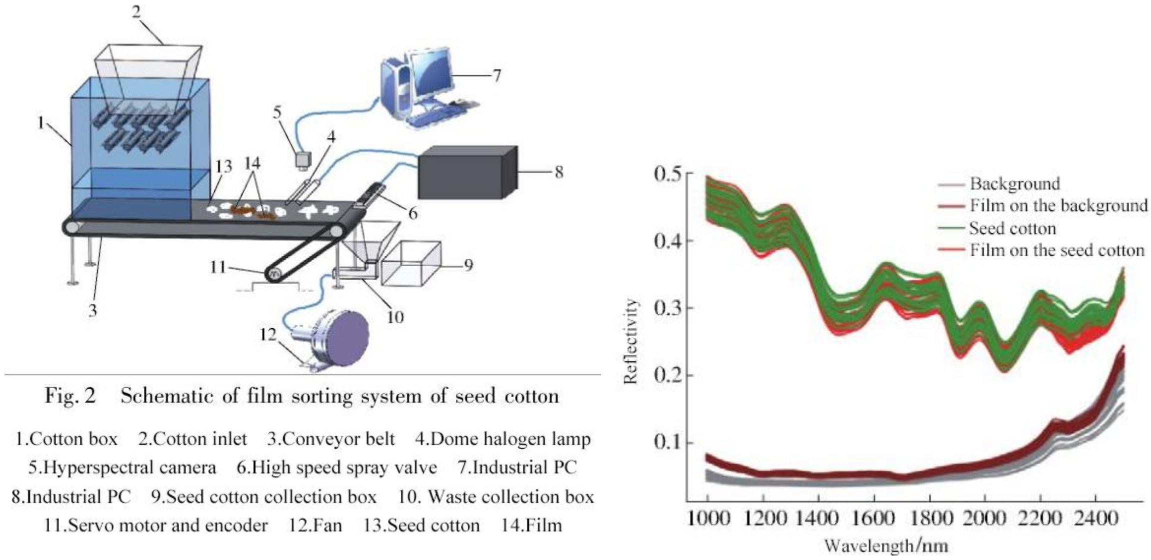

Figure 12 Seed cotton sorting application; (a) System functional composition; (b) Different substances reflectance spectrum

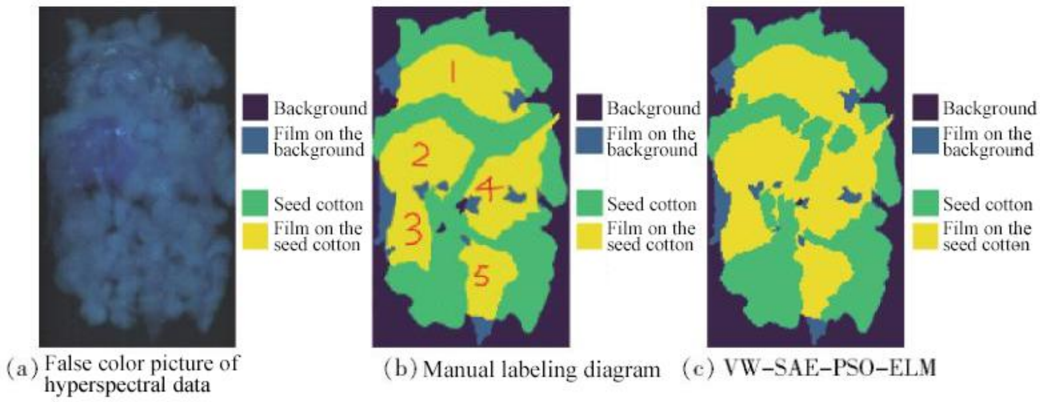

Figure 13 Seed cotton sorting application; (a) Artificial marking; (b) Recognition result

Apple's external quality is the most intuitive quality feature of Apple, which directly affects Apple's price and consumer preference. Aiming at the difficulties and key points of external inspection of apples, based on machine vision technology, hyperspectral imaging technology and multispectral imaging technology, integrated image processing technology, pattern recognition method, chemometric method and spectral analysis technology, the external physical quality of apple (shape and size) and detection methods for common defects on the surface.

The detection system and algorithm developed on the basis of the above research laid the foundation for my country's research and development of rapid online inspection and grading equipment for Apple's external quality based on machine vision technology and multi-spectral machine vision technology.

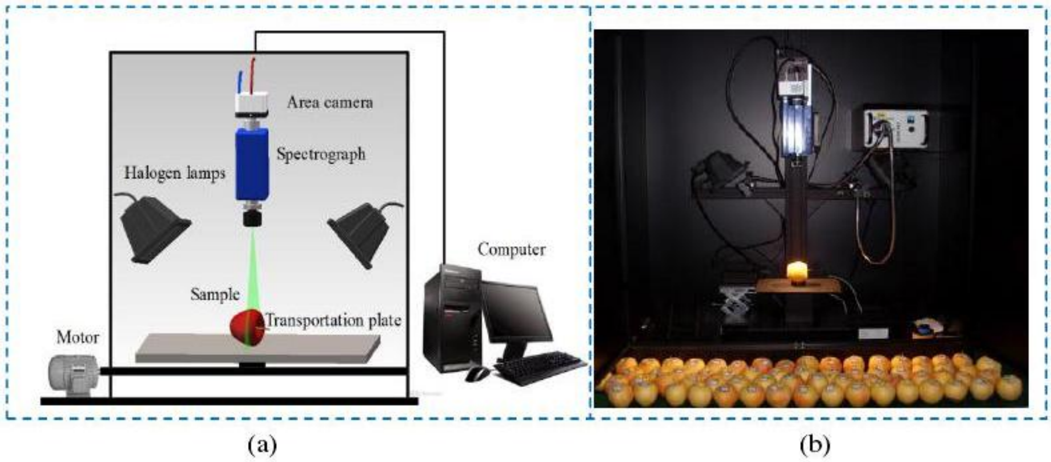

Figure 14 Schematic diagram and physical diagram developed by Dr. Zhang Baohua of Shanghai Jiaotong University; (a) Schematic diagram; (b) Physical diagram

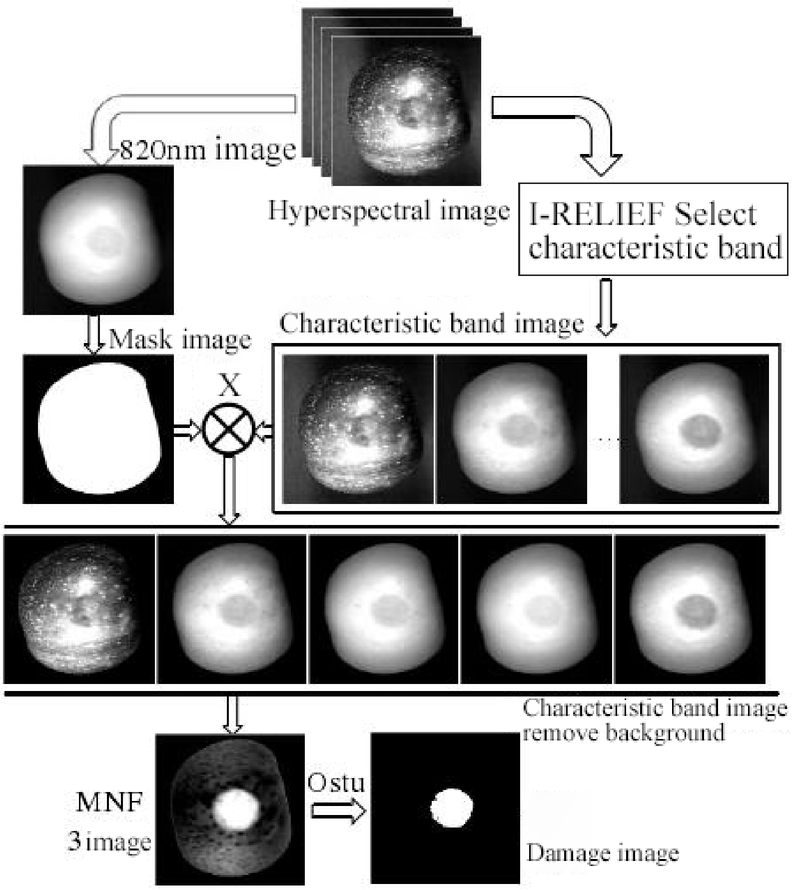

Figure 15: Flow chart of early damage detection algorithm for apple surface

1503 Bld. A04, 3rd Software Park, Jimei, Xiamen, 361005, China
Tel: +86-592-6102588

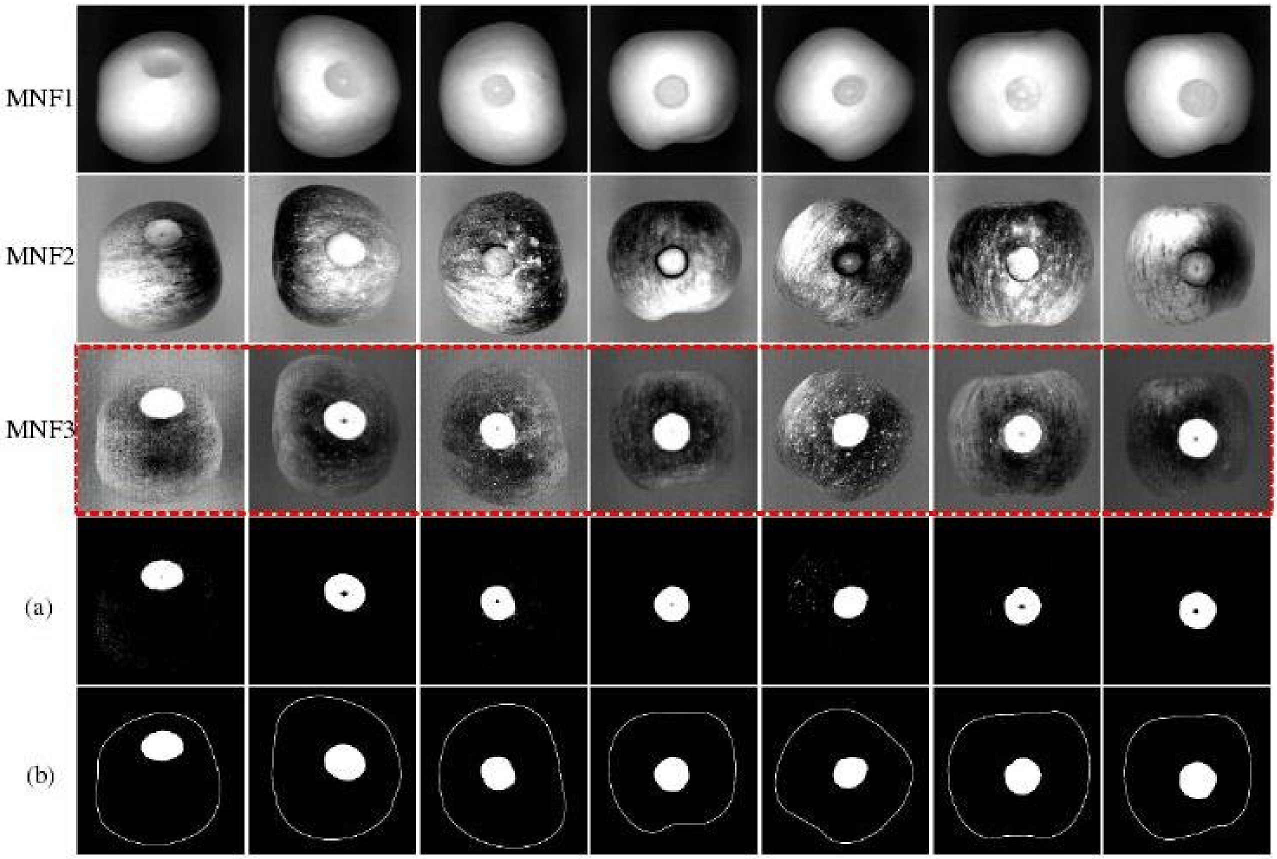

Figure 16 Recognition results of early decay of some apples and intermediate processing (a) rot segmentation results (b) final results

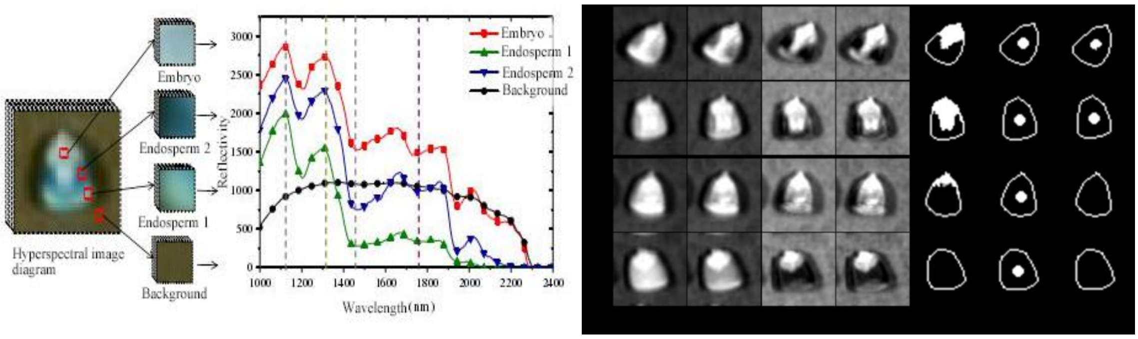

Figure 17 Corn seed sorting application (Dr. Chaopeng Wang, Northwest A&F University)

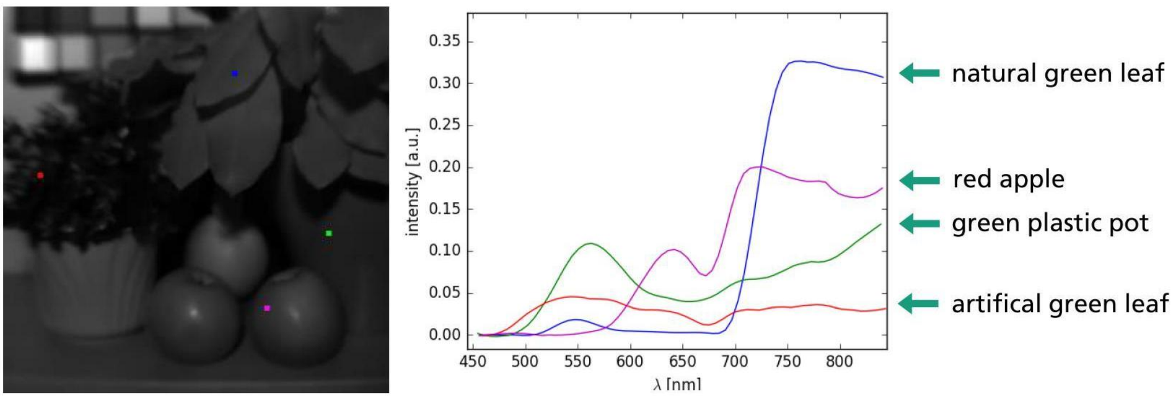

Figure 18 The spectrum of natural green plants, artificial green leaves, green plastic, and red apples

1503 Bld. A04, 3rd Software Park, Jimei, Xiamen, 361005, China
Tel: +86-592-6102588

5.2 Precision Agriculture Application

Figure 16 Drone-borne hyperspectral imaging camera

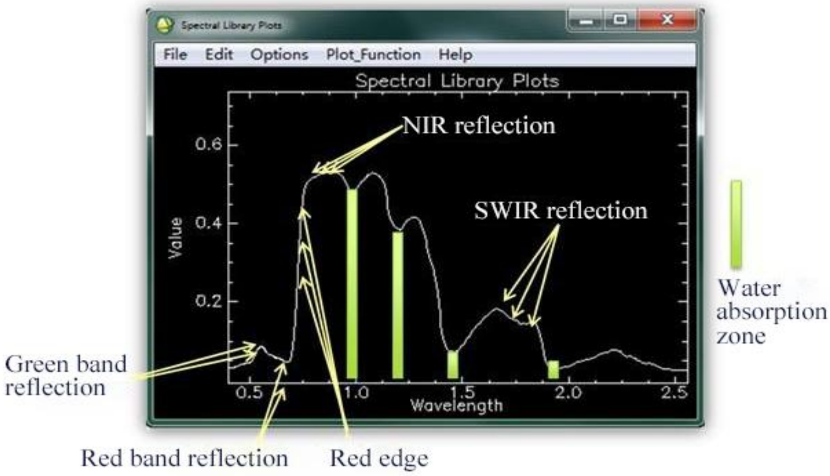

Figure 17 Green plants measured spectrum

1) **Crop growth monitoring and yield estimation:** Due to the different external factors of crops at each stage of their growth and development, there will be certain differences in their internal composition and external morphology. The most important difference is the leaf area index. Leaf area index is a comprehensive index reflecting the individual characteristics and group characteristics of crops.
2) **Crop pest control:** Remote sensing technology can monitor the effects of pests and diseases on the growth and development of crops, track the growth and development of crops, analyze and estimate disaster losses, and can monitor the distribution and activity of pests, thereby preventing the occurrence of pests.
3) **Drought monitoring of crops:** Remote sensing technology monitors crop drought conditions through crop vegetation index and canopy parameters.
4) **Monitoring of soil moisture content and distribution:** In the case of different thermal inertia

conditions, the difference between remote sensing spectra is very obvious, so a mathematical model between thermal inertia and soil moisture content can be established, and remote sensing technology uses this model to analyze soil moisture content and distribution.

5) **Crop nutrient monitoring:** The accuracy of remote sensing technology to monitor the nitrogen content of crops is higher than that of other nutrient elements.

Normalized difference spectral index (NDSI), ratio spectral index (RSI) and simple spectral index (SSI) were constructed by using single band and any two bands in the range of 450 ~ 882 nm to calculate the correlation between CGI and spectral index and screen out spectral index with good correlation. Combined with partial least squares regression (PLSR), the inversion model was established.

Using CGI as the index, Airborne hyperspectral image was used to monitor the growth status of wheat in the multi-growth period in 2015. Unmanned aerial vehicle hyperspectral image inversion CGI has high precision, which can judge the difference of wheat overall growth, and can provide reference for wheat growth monitoring.

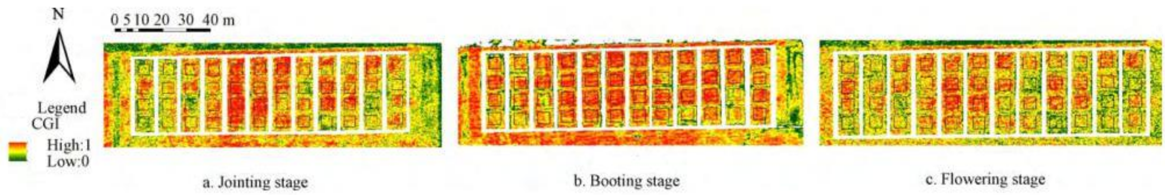

Figure 18 CGI inversion of wheat growth index

5.3 Forest Health Application

Used for pest monitoring and forest resource assessment.

Principle: The health of vegetation is related to greenness index, leaf area index, leaf moisture content and light use efficiency;

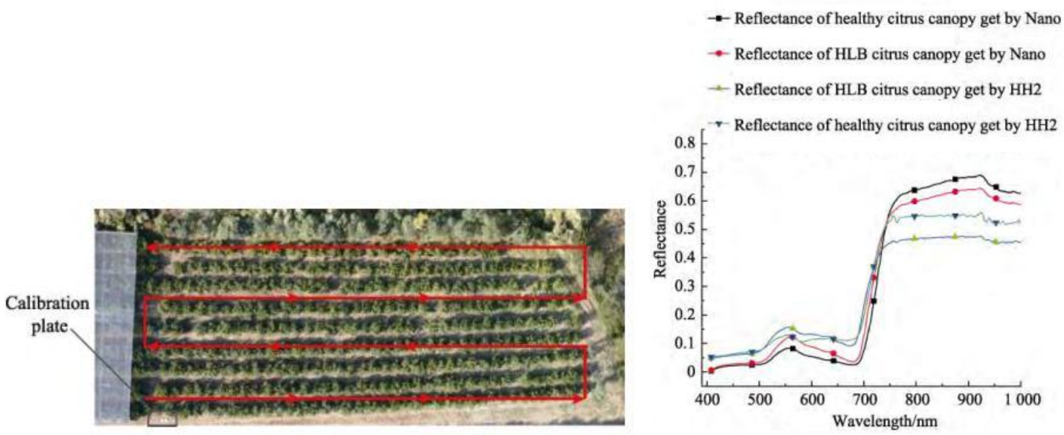

Figure 19 Monitoring and classification of citrus yellow dragon disease plants based on drone-borne hyperspectral imaging camera (designed by Lan Yubin et al., South China Agricultural University)

1503 Bld. A04, 3rd Software Park, Jimei, Xiamen, 361005, China
Tel: +86-592-6102588

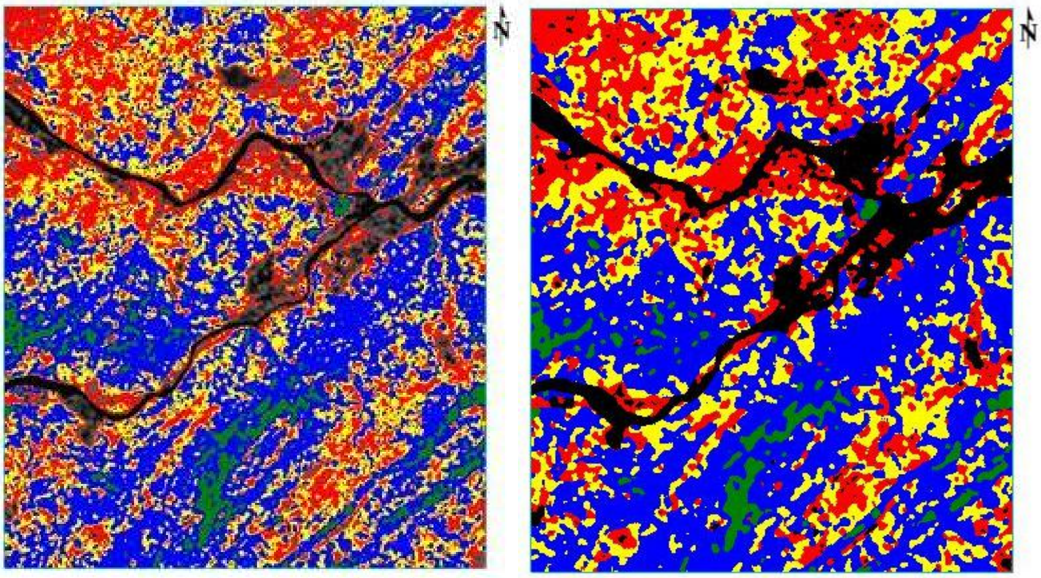

Figure 20 Distribution map of masson pine health degree studied by Wang Shuang of the University of Electronic Science and Technology of China with a hyperspectral camera

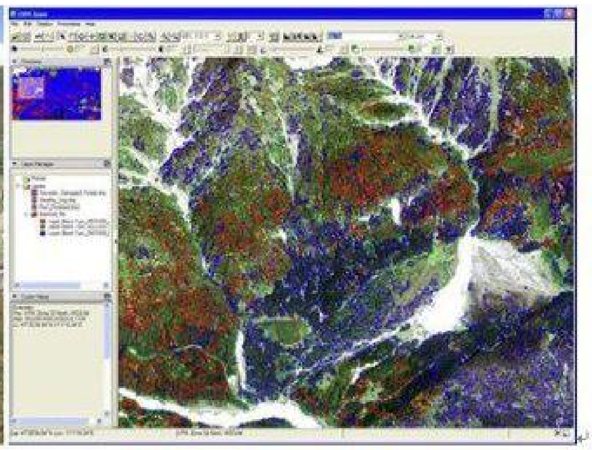

5.4 Geological Prospecting Application

Spectral remote sensing technology evolved from the multi-spectral remote sensing technology represented by Landsat and took initial shape in the mid-1980s (Goets et al., 1985, Tong Qingxi et al., 2006).

Due to its advantages of high spectral resolution and atlas integration, hyperspectral remote sensing technology has the ability of fine detection and analysis of surface rock mineral composition on a large scale. It can not only provide a macro image of the ground, but also determine the type and abundance of minerals in the geological body, and even the chemical composition of some minerals at pixel level details (Wang Runsheng et al., 2010).

In recent years, with the continuous development of hardware, data processing methods and software related to imaging spectrometer, the application of hyperspectral remote sensing technology in the field of geological survey has been accelerated.

Hyperspectral remote sensing technology has played an important role in geological mapping, the definition and division of hydrothermal alteration zones, and the delineation and discrimination of

1503 Bld. A04, 3rd Software Park, Jimei, Xiamen, 361005, China
Tel: +86-592-6102588

mineralization anomalies from large metallogenic areas to medium-scale ore fields (e.g. Bierwirth et al., 2002; Company Changyun et al., 2005; Kruse et al., 2006; Cudahy et al., 2007; Wang Runsheng et al., 2010; Liu Dechang et al., 2011; Yan Baikun et al., 2014; Yang Zian et al., 2015; Graham et al., 2017).

With the theory of metallogenic system (Wyborn et al., 1994) becoming the guiding principle of prospecting practice, thematic mineral mapping on the scale of large ore concentration areas and metallogenic belts will provide key regional material composition information for predictive prospecting and exploration.

The spectral wavelength ranges used for mineral mapping include visible light (400-700nm), NIR (700-1000nm), SWIR (1000-2500nm), and thermal IR (7000-15000nm). At present, the most widely used in mining is the short-wave infrared region (1000-2500nm).

Because the frequency is close to the cofrequency and combined frequency of the chemical bond vibration in the mineral lattice, the mineral containing water or OH- (mainly layered silicate and clay) as well as some sulfate and carbonate minerals can be observed in the range of short-wave infrared wavelength.

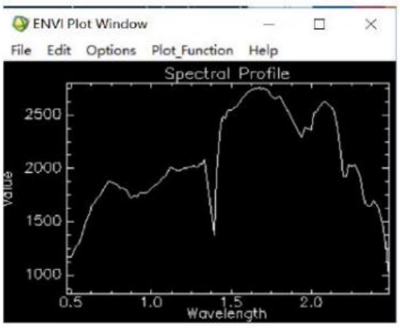

HH036 point image spectrum

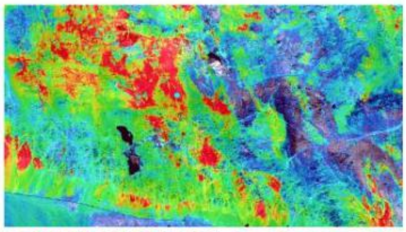

Sericite Filling Results Comparison of known deposit points between HH036 and measured

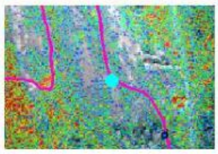

Chlorite extraction results

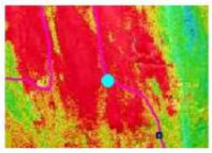

Sericite extraction results

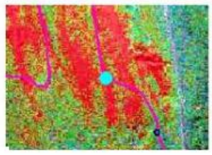

Feb3+ extraction result

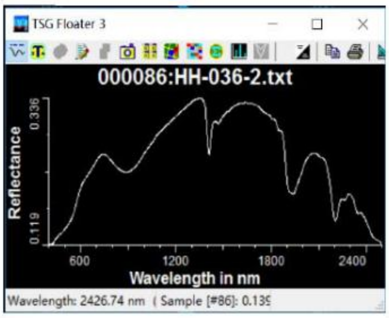

HH036 point measurede spectrum

Sampling point photos

Long-range photos of sampling points

1503 Bld. A04, 3rd Software Park, Jimei, Xiamen, 361005, China
Tel: +86-592-6102588

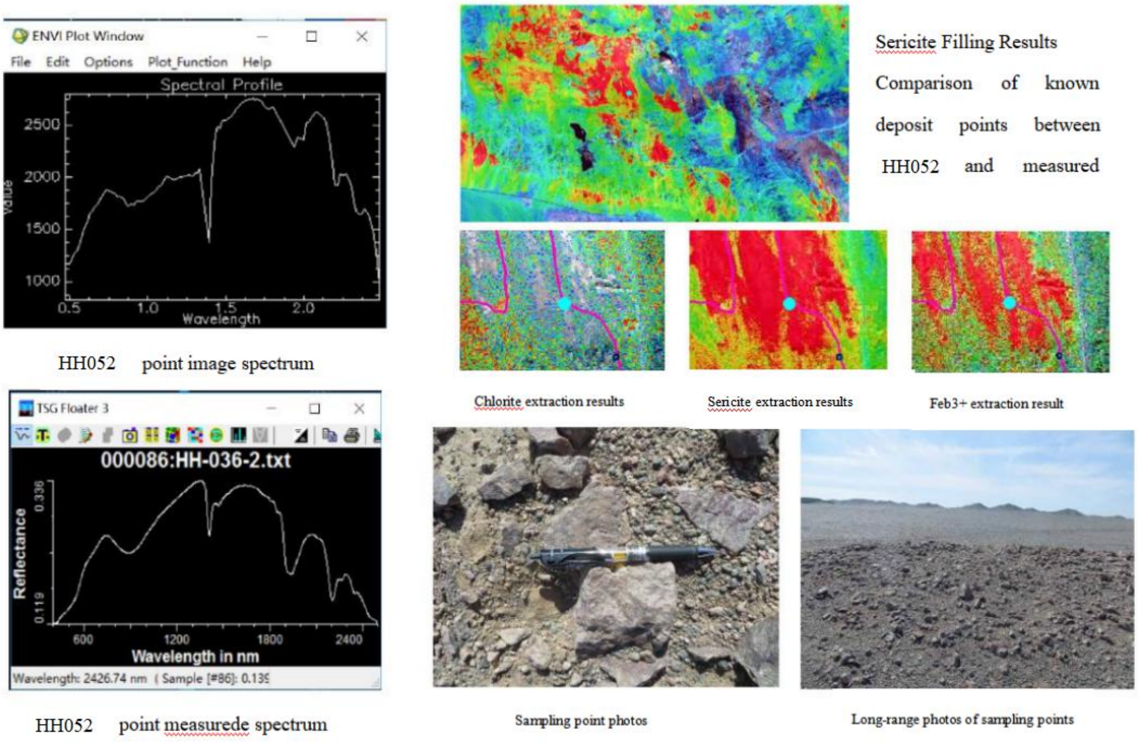

Figure 21 Application of hyperspectral imager in prospecting

Soil salinization is one of the important ecological and environmental problems in arid and semi-arid areas. Soil salinization causes soil hardening, fertility decline, acid-base imbalance, land degradation and other consequences, which seriously restricts agricultural development in China and affects the strategic situation of sustainable development in China at present.Remote sensing technology, with its characteristics of large scale, wide range, strong timeliness and economy, makes up for the deficiency of traditional methods for monitoring salinization phenomenon, and provides a new way for quantitative monitoring of soil salinization phenomenon.

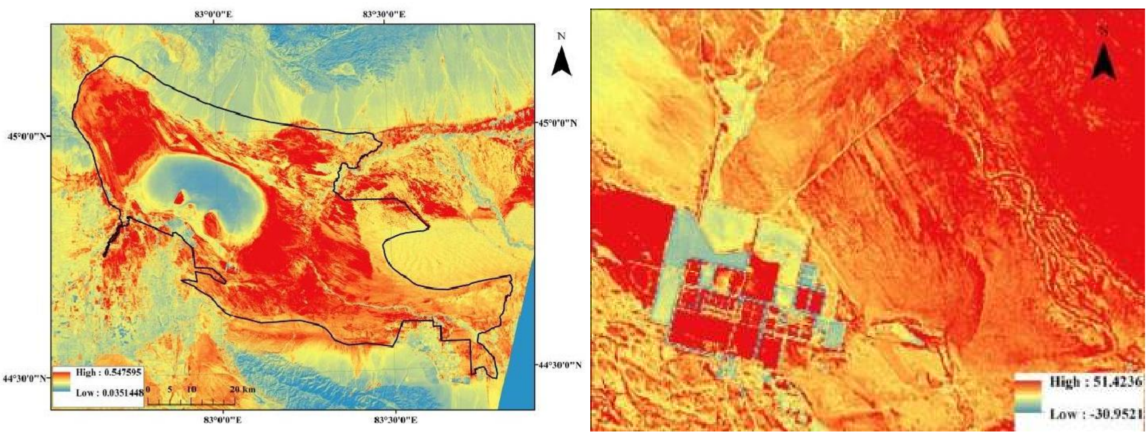

Figure 22 The surrounding area of a salt field

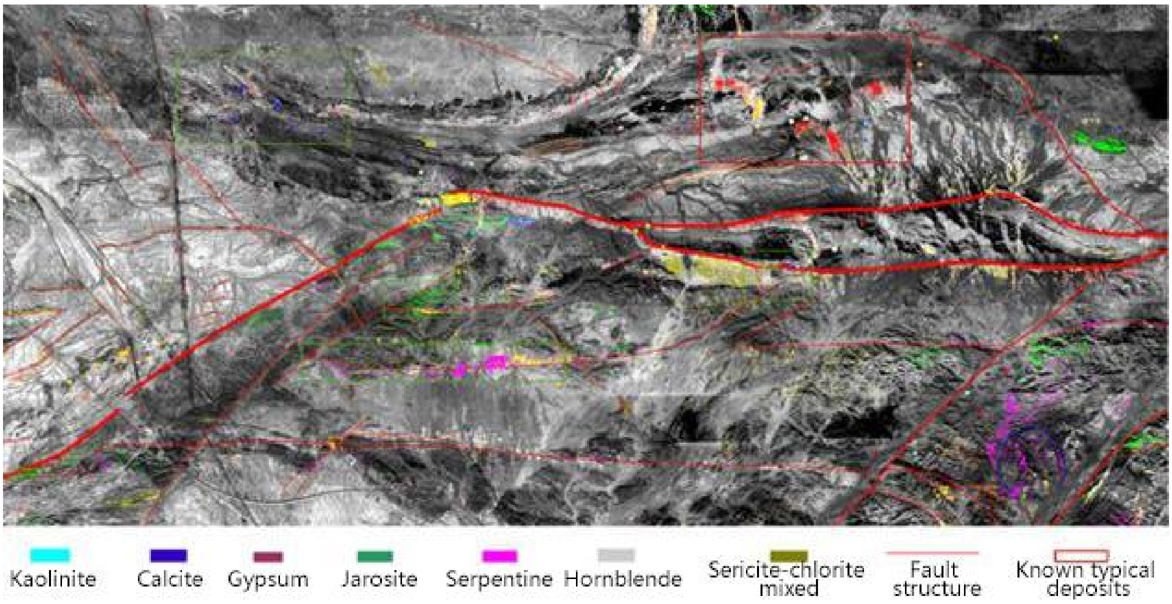

5.5 Public Safety Application

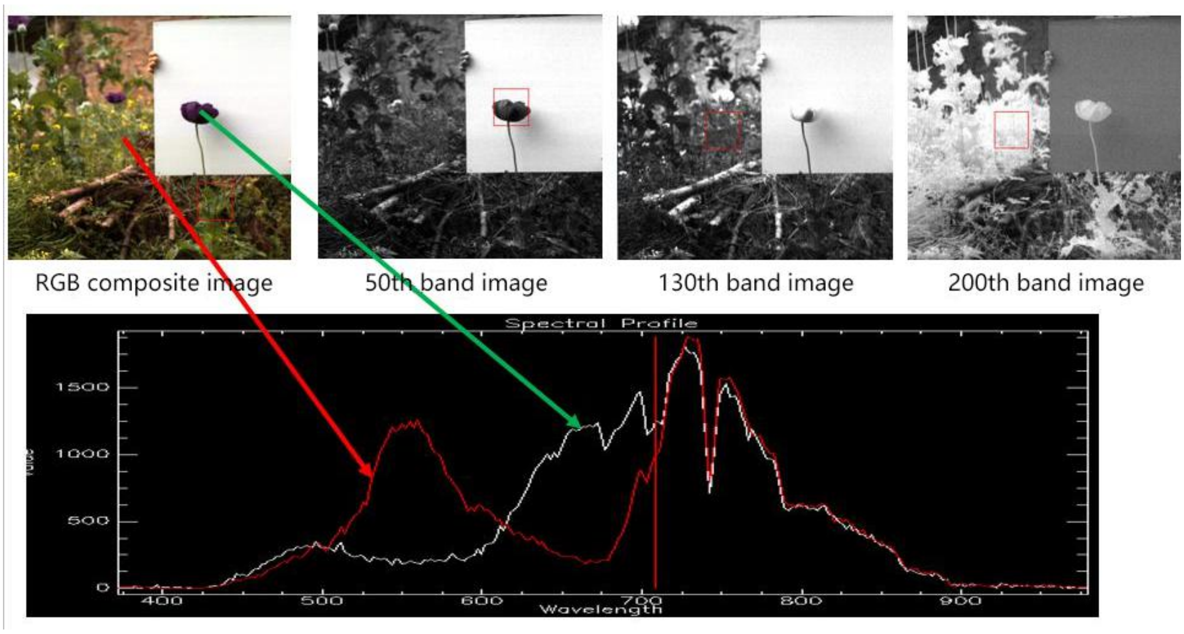

Figure 23 The searching for illegal poppy cultivation application

Figure 24 Document inspection application

5.6 Medical Microscopic Imaging Application

Objective: online detection and navigation positioning during tumor surgery

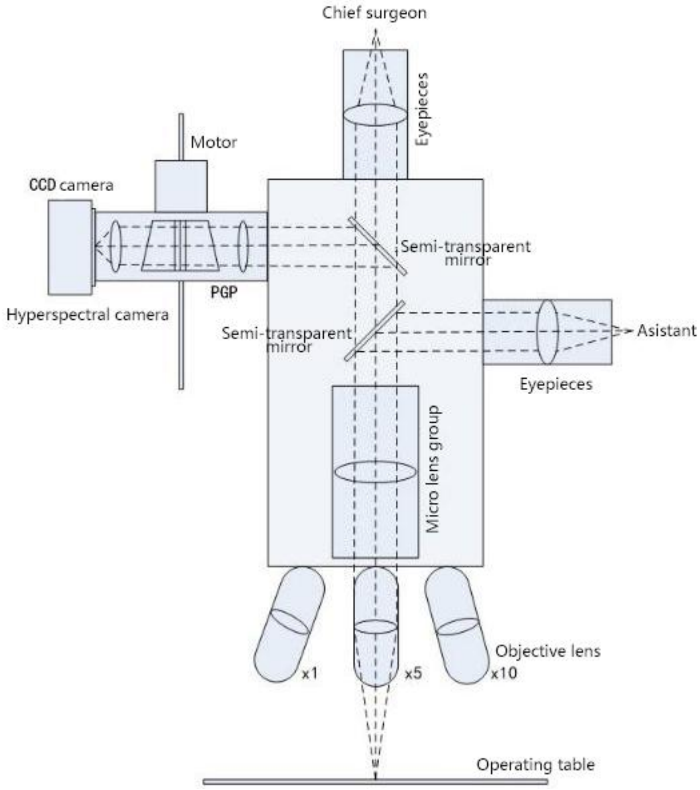

Figure 25 Medical microscope imager optical path schematic diagram

Is shown in the figure of medical microscopic imaging spectrometer principle diagram, the operating table for the target after the objective lens, microscope lens group is divided into three road, visual observation for the surgeon, all the way all the way for the assistant auxiliary visual observation, a routing imaging spectrometer detection, driven by a motor to imaging spectrometer measuring target space d scanning, imaging spectral information of the target under test, then through data analysis, image processing, through the display to the doctor.

1503 Bld. A04, 3rd Software Park, Jimei, Xiamen, 361005, China
Tel: +86-592-6102588

Figure 26 Medical microscope imager figure

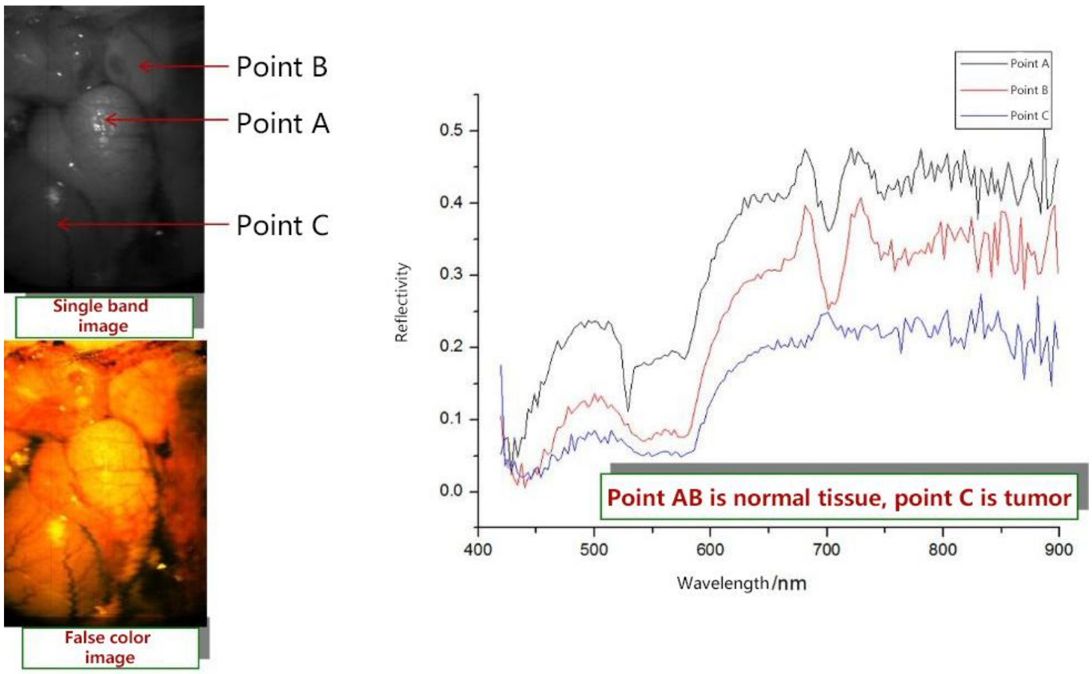

Figure 27 Data collect by medical microscopic imager

5.7 Airborne Imaging Spectroscopy Application

Figure 28 Optosky Airborne Imaging Camera

Objective: Airborne remote sensing

Application: Figure shows airborne imager consists of SpecVIEW-VIS, stable platform and POS modules. Figure 30 and Figure 31 show data was collecte. Figure 7 shows pseudo color image processed through geometric correction, flight strip spice and radiatation correction. Figure 31 shows typical geology spectral curve.

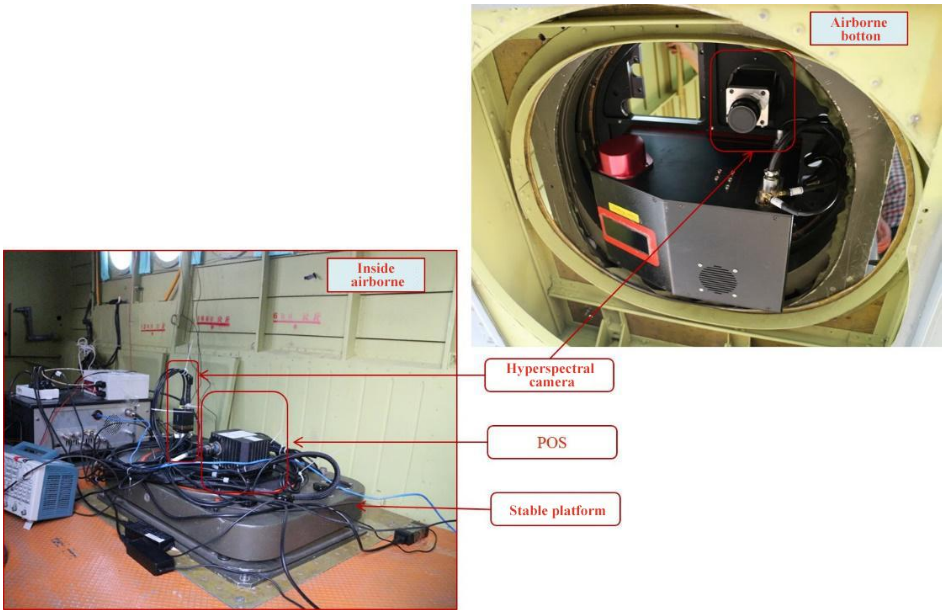

Figure 29 Airborne remote sensing application

1503 Bld. A04, 3rd Software Park, Jimei, Xiamen, 361005, China
Tel: +86-592-6102588

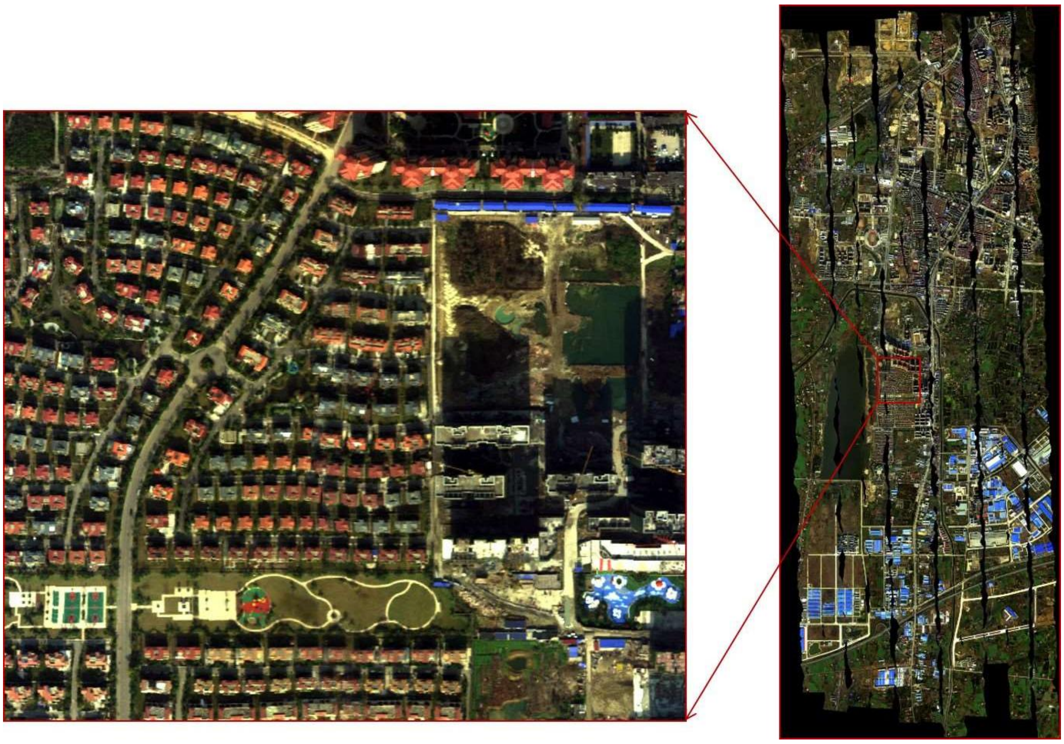

Figure 30 Airborne application data-pseudocolor image

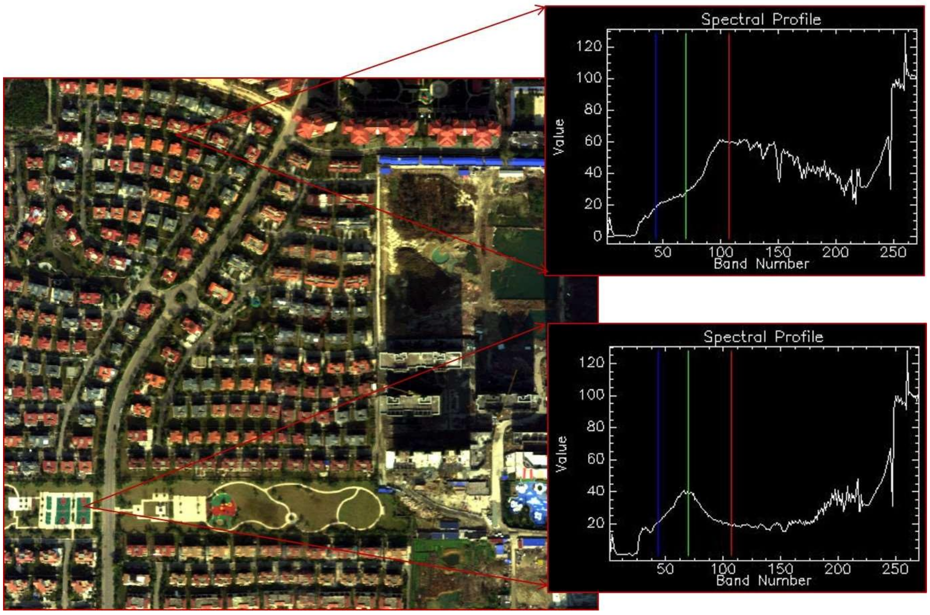

Figure 31 Airborne application data-spectral curve

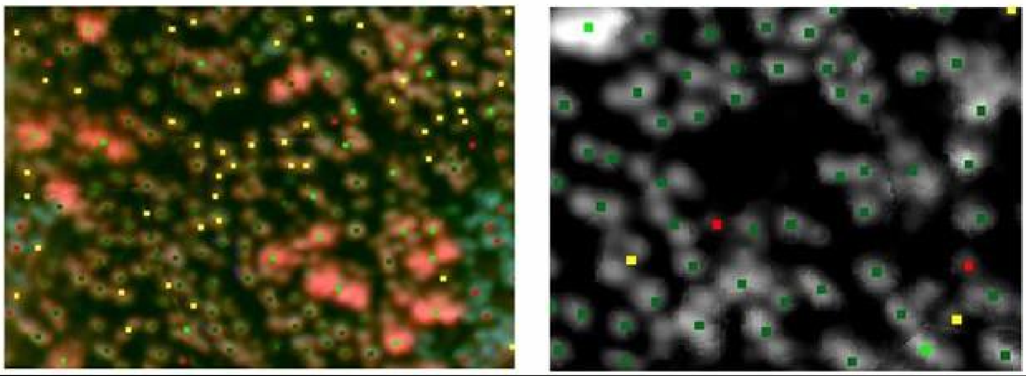

1503 Bld. A04, 3rd Software Park, Jimei, Xiamen, 361005, China
Tel: +86-592-6102588

Figure 32 Forest remote sensing, Airbone hyperspectral monitor forest disease and pest

5.8 Water Quality and Environmental Protection Appication

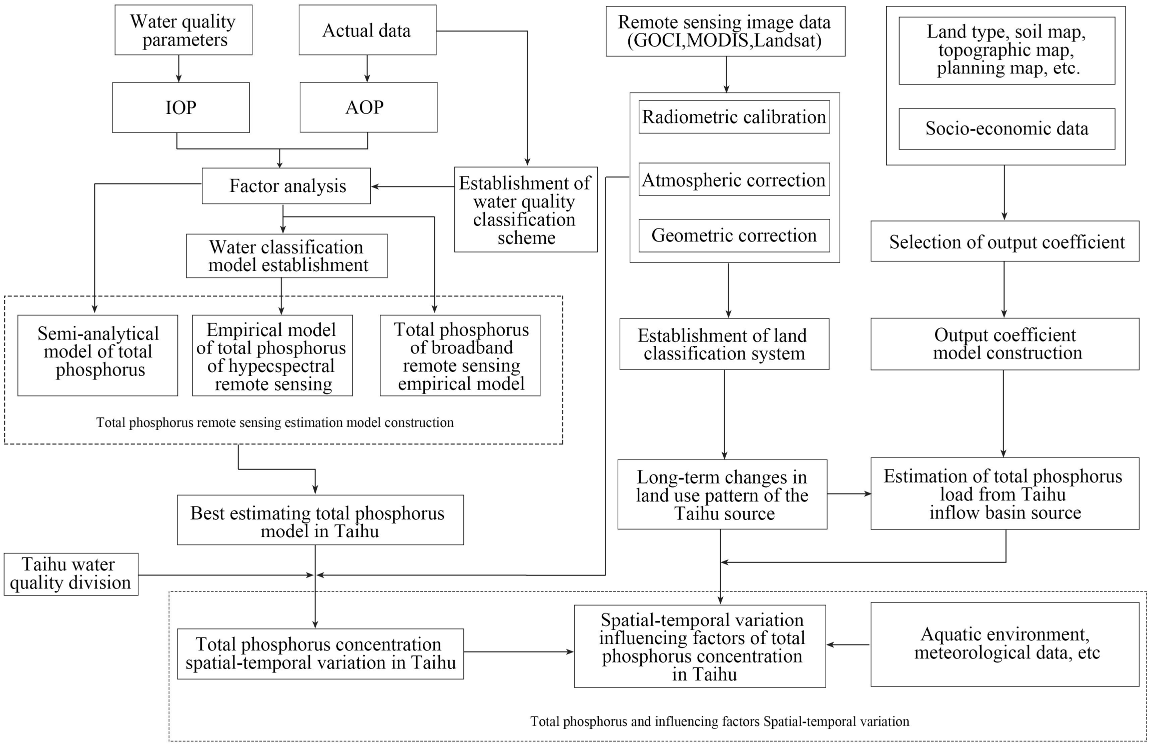

Figure 33 Inversion algorithm flow of hyperspectral data

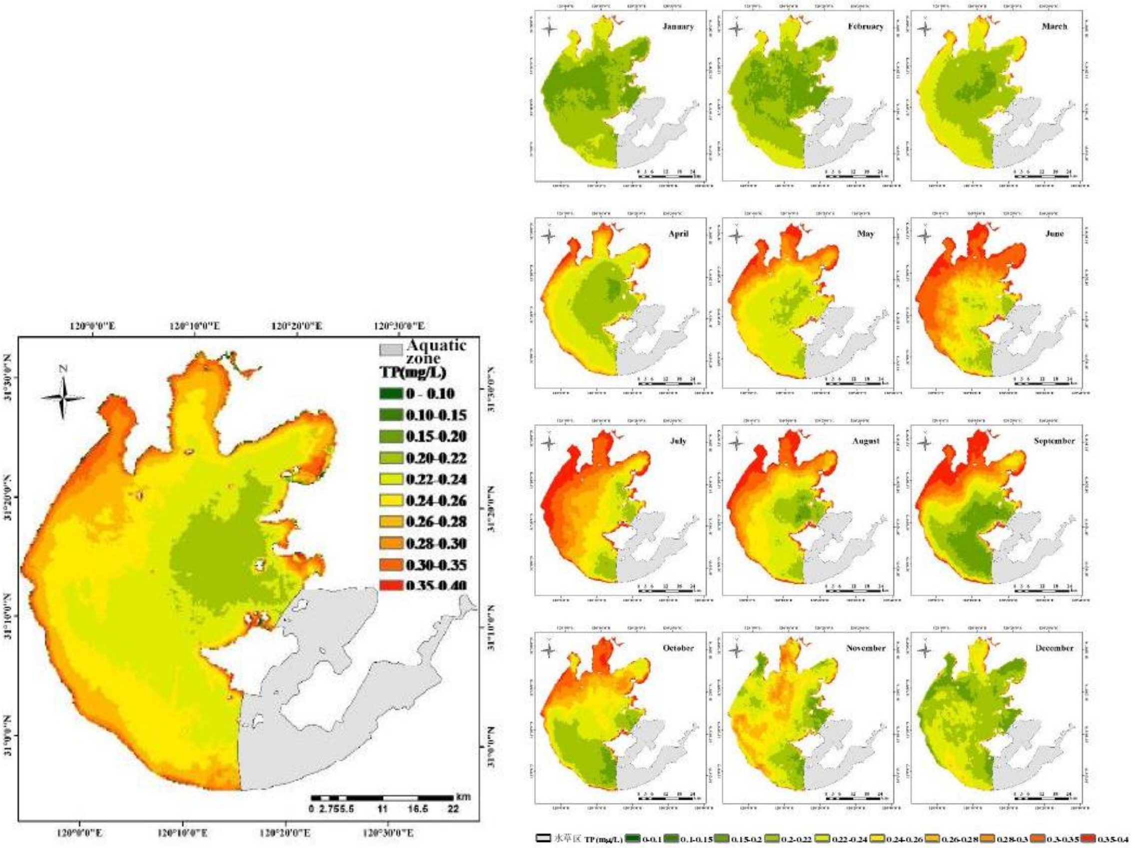

Fig. 34 (a) Spatial distribution of total phosphorus concentration in Taihu Lake. The spatial difference of total phosphorus concentration was obvious, with the highest value of 0.38mg/L and the lowest value of 0.06mg/L. (b) Monthly variation of total phosphorus concentration in different lakes.

The lake area also generally reaches its maximum phosphorus concentration between June and September. The total phosphorus concentration in Zhushan Bay, Meiliang Bay and the west bank of Taihu Lake was higher than the mean value of the whole lake from March to October of the year, and was significantly higher than that in the rest of Taihu Lake. The total phosphorus concentration in Gonghu Bay was higher than that in the whole lake only in June, and the total phosphorus concentration in the south bank of Taihu Lake and Great Taihu Lake was relatively low throughout the year.

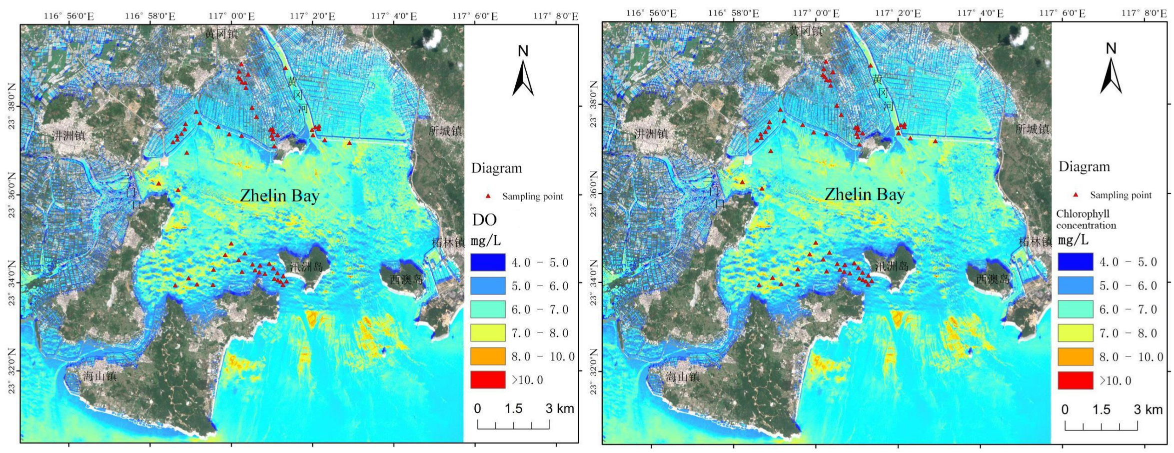

Figure 35 The distribution of dissolved oxygen and chlorophyll concentration in Zhelin Bay, eastern Guangdong, taken by hyperspectral

1503 Bld. A04, 3rd Software Park, Jimei, Xiamen, 361005, China
Tel: +86-592-6102588